# The Physics of Broadcast Spawning in Benthic Invertebrates

John P. Crimaldi[1] and Richard K. Zimmer[2]

[1]Department of Civil, Environmental, and Architectural Engineering, University of Colorado, Boulder, Colorado 80309-0428; email: crimaldi@colorado.edu

[2]Department of Ecology and Evolutionary Biology, University of California, Los Angeles, California 90095-1606; email: z@biology.ucla.edu

Annu. Rev. Mar. Sci. 2014. 6:141–65

First published online as a Review in Advance on August 14, 2013

The *Annual Review of Marine Science* is online at marine.annualreviews.org

This article's doi:
10.1146/annurev-marine-010213-135119



## Keywords

fertilization, turbulence, sperm, egg, flow, chemoattractant

## Abstract

Most benthic invertebrates broadcast their gametes into the sea, whereupon successful fertilization relies on the complex interaction between the physics of the surrounding fluid flow and the biological properties and behavior of eggs and sperm. We present a holistic overview of the impact of instantaneous flow processes on fertilization across a range of scales. At large scales, transport and stirring by the flow control the distribution of gametes. Although mean dilution of gametes by turbulence is deleterious to fertilization, a variety of instantaneous flow phenomena can aggregate gametes before dilution occurs. We argue that these instantaneous flow processes are key to fertilization efficiency. At small scales, sperm motility and taxis enhance contact rates between sperm and chemoattractant-releasing eggs. We argue that sperm motility is a biological adaptation that replaces molecular diffusion in conventional mixing processes and enables gametes to bridge the gap that remains after aggregation by the flow.

## 1. INTRODUCTION

Interdisciplinary studies of complex ecological systems in marine science are increasingly considering physical-biological interactions between organisms and their flow environments (e.g., see the reviews Nowell & Jumars 1984, Abelson & Denny 1997, Hart & Finelli 1999, Webster & Weissburg 2009, Denny & Gaylord 2010, Guasto et al. 2012). In examining an ecological process controlled by both the physics of fluid flow and the biology of sexual reproduction, the study of broadcast spawning in benthic invertebrates exemplifies this duality.

Fertilization is the bridge between generations. Although it has been studied for more than a century, it remains one of the least understood fundamental biological processes. Most benthic invertebrates spawn their gametes into the sea, and sexual union occurs externally to female reproductive tracts. For these free-spawning organisms, external fertilization is a complex interaction among biological traits of gametes and physical properties of the ocean environment. It is generally considered a two-step process: First, male and female gamete clouds are stirred by the fluid flow, and second, sperm contact and penetrate an egg. The exact contributions of larger-scale (stirring of gamete plumes) and smaller-scale (sperm-egg encounters) processes to fertilization success have not been established for even a single species. Although considerable progress has been made over the past 30 years, studies have yet to link critical physical and biological mechanisms that pertain to the production, release, and transport of spawned materials or to microscopic interactions among individual gametes. New research, however, is poised to establish these linkages. The next 10 years should see major advancements in understanding sex in the sea.

## 2. BROADCAST SPAWNING IN BENTHIC INVERTEBRATES

Sexual reproduction plays a vital role in the exchange of genetic material as well as in the demographic processes and community dynamics of marine benthic invertebrates. For example, the complex life cycles of many species involve a sessile (or sedentary) adult and dispersing gametes (products of broadcast spawning) and juveniles. Local demes, established and maintained by scattering zygotes, embryos, and larval propagules, often form patch mosaics within metapopulations. At a given site, species-specific dispersal patterns create population templates that can strongly influence community structure (Gaines & Bertness 1992, Caley et al. 1996, Eckman 1996, Underwood & Keough 2001, Gaylord et al. 2006). These patterns also characterize the rate of population growth and spreading and the degree of persistence in patchy environments. For externally fertilizing organisms, the timing and magnitude of larval supply depend on the timing and magnitude of external spawning events (Morgan & Christy 1994, Hughes et al. 2000). Fundamental demographic processes of birth and immigration can covary. The magnitude of success in external fertilization (either locally or regionally within a metapopulation) sets an initial upper limit to recruitment even if zygotes, embryos, and larvae are transported away from adult source (spawning) populations as a consequence of ocean currents and mixing. Thus, broadcast spawning determines gamete availability, and physical and biological processes determine fertilization success, the first limiting step in life cycle dynamics.

External fertilization incorporates the synchronous release of sperm and eggs from separate locations, whereupon the process depends on structured stirring by the flow field (at large scales) and sperm motility and taxis (at small scales) to bring the gametes together (Crimaldi 2012). To spawn, adults release sperm and eggs into the ocean. For fertilization to take place, concentrated parcels of male and female gametes must come into close proximity, and stirring by ambient flow is certain to play an important role in this process (Pennington 1985, Denny & Shibata 1989, Babcock et al. 1994, Metaxas et al. 2002).

A variety of physical, chemical, and biological factors are key to fertilization success in broadcast-spawning organisms. Field experiments (Pennington 1985, Atkinson & Yund 1996, Coma & Lasker 1997, Levitan 2005) and analytical models (Denny et al. 1992, Claereboudt 1999, Lauzon-Guay & Scheibling 2007) have shown that adults aggregate and are distributed to concentrate their gametes, enhancing the likelihood of fertilization. Adult synchronization of gamete release also improves the probability that sperm contact eggs and reduces the impacts of gamete aging (Giese & Pearse 1974, Levitan 1995, Lauzon-Guay & Scheibling 2007). Fertilization success is additionally influenced by the temporal dynamics of gamete release (Benzie & Dixon 1994), individual reproductive output, and the collective ratio of sperm and eggs (Yund 2000). Once released into the water column, male and female gametes may initially comingle as a result of passive transport by turbulence (Crimaldi & Browning 2004). Eventually, however, strong turbulent stirring and mixing produce long-term dilution of gamete concentrations (Csanady 1973, Denny et al. 1992). Such dilution may be mitigated when gametes are released in a viscous matrix (Thomas 1994b, Marshall 2002, Yund & Meidel 2003) or when adults aggregate and gametes are sequestered at sites of relatively slow flow (Pearson & Brawley 1996, Riffell & Zimmer 2007).

Recent efforts to model broadcast-spawning fertilization rates have been based on the fertilization kinetics model developed by Vogel et al. (1982) or extensions of it that incorporate effects of polyspermy (Styan 1998, Styan & Butler 2000, Millar & Anderson 2003), gamete covariance (Luttikhuizen et al. 2004), or incomplete fertilization (Hodgson et al. 2007). The simplest kinetics model corresponds to that of a bimolecular reaction between two scalar concentrations ($C_E$ and $C_S$ for egg and sperm, respectively). The likelihood of an individual egg being fertilized is dependent on sperm concentration, and the resulting dimensional rate at which "virgin" eggs are fertilized is (Denny & Shibata 1989)

$$\Theta_E = \Phi C_E C_S. \quad (1)$$

Likewise, the rate at which viable sperm are removed by fertilization is

$$\Theta_S = \phi C_E C_S. \quad (2)$$

The rate constants $\Phi$ and $\phi$ for egg and sperm may differ by several orders of magnitude, because many sperm that attach to eggs do not result in fertilization.

Gamete size, motility, and sensory abilities contribute further to broadcast-spawning success. When fertilization is chronically limited by sperm availability, adults and gametes are under selection for mechanisms that increase sperm-egg contact (Levitan 1995, Podolsky 2001, Levitan 2006). One such mechanism involves changes in egg size. Enlarging the target increases the probability of sperm-egg collision (Cox & Sethian 1985, Levitan 1993). Models of evolution have traditionally focused on postzygotic consequences of egg size for larval or juvenile survival (Strathmann 1985, Havenhand 1993, Marshall et al. 2003, McEdward & Miner 2006). There are also (or can alternatively be) prezygotic benefits to external fertilization success that drive the evolution of egg size and, in turn, anisogamy (Hoekstra 1987, Levitan 1993, Dusenbery 2006).

Egg cytoplasm is an expensive commodity. It contains a vast array of organic molecules and provides a rich biochemical environment for synthesizing natural products after fusion, as required for reproductive success (Jaeckle 1995). There are thus cheap evolutionary alternatives that enhance egg target size without enlarging cytoplasmic and/or cellular volume. Chemical communication, for one, is common among the gametes of taxa with diverse reproductive strategies (Miller 1985, Olson et al. 2001, Spehr et al. 2003). Sperm activation and chemotaxis (orientation with respect to a chemical concentration gradient) occur in benthic animals and plants that broadcast gametes into the sea (Ward et al. 1985, Maier & Müller 1986, Miller & Vogt 1996, Yoshida et al. 2002). At the spatial scale of gamete interactions (0.01–1 mm with a Reynolds number of 1, where the

latter is a dimensionless ratio that reflects the magnitude of inertial to viscous forces that act on a body in flow), sperm encounter eggs while being transported within a laminar shear flow (Karp-Boss et al. 1996, Mann & Lazier 1996). The free amino acid L-tryptophan, for example, acts as a natural chemoattractant to promote sperm-egg encounter rate and fertilization success in red abalone (*Haliotis rufescens*) (Riffell et al. 2002). During oogenesis, this substance is taken up by the maternal abalone from a dietary source and incorporated directly into the egg (Krug et al. 2009). Chemoattractant production and release therefore consume little or no metabolic energy. At low shears, fertilization success (proportion of fertilized eggs) is highly correlated with the strength of sperm chemotaxis in response to the natural L-tryptophan cue (Zimmer & Riffell 2011). Other accessory structures surrounding an egg, such as the jelly coat—a fibrous network of (mostly) carbohydrate strands and globular proteins—further facilitate gamete interaction at little cost and increase the likelihood of fertilization (Mozingo et al. 1995, Vacquier & Moy 1997, Bolton et al. 2000, Podolsky 2004). In fact, for some species, the chemoattractant is associated explicitly with the jelly coat (Ward et al. 1985). For others, carbohydrate strands may trap or collect sperm, or may redirect sperm swimming paths toward the egg through an unknown mechanism (Reinhart et al. 1998, Farley & Levitan 2001, Podolsky 2001).

Over the past 30 years, there has been an impressive accumulation of knowledge on mechanisms pertaining to broadcast spawning. Generally lacking, however, is cohesion among findings from separate studies on physical, chemical, and biological aspects of external fertilization. Here, we coalesce these results and strive to bridge the gaps between disciplines. The object is to create a new synthesis that ties together processes at macroscopic and microscopic scales, creating a single continuum. This new integration begins with adult release of gametes and their hydrodynamic transport in plumes, and ends with the behavioral events that ultimately lead to final contact between an individual sperm and egg.

## 3. MEAN GAMETE DISPERSION

Two simplifications are often invoked when modeling gamete dispersion and fertilization downstream of adults. The first simplification is that gametes are advected by the flow in the same fashion as passive solutes. This eliminates the complexities of how gamete size, shape, buoyancy, rheology, and motility alter the details of turbulent transport. The second simplification is that the fertilization rate can be estimated based only on knowledge of the mean (time-average) gamete distributions. This eliminates the need to know the complex spatial and temporal structure of the instantaneous flow and its effect on instantaneous gamete distributions. Instead, the aggregate effect of macroscopic turbulent fluctuations on mean plume dispersion is modeled by an effective turbulent or eddy diffusivity that is much greater than any diffusivity resulting from microscopic processes (e.g., Shraiman & Siggia 2000). In the simplest implementation, the effective diffusivity has a single value, meaning that spatial variations in mixing efficiency resulting from boundary-layer inhomogeneity and anisotropy (Crimaldi et al. 2002) or from bed roughness and topography (Rahman & Webster 2005) are ignored.

For a homogeneous anisotropic turbulent flow with mean velocity $U$ in the $x$ direction, the concentrations of virgin egg ($C_E$) and sperm ($C_S$) are governed by (Crimaldi & Browning 2004)

$$\frac{\partial C_E}{\partial t} = -U\frac{\partial C_E}{\partial x} + D_y\frac{\partial^2 C_E}{\partial y^2} + D_z\frac{\partial^2 C_E}{\partial z^2} - \Theta_E \tag{3}$$

and

$$\frac{\partial C_S}{\partial t} = -U\frac{\partial C_S}{\partial x} + D_y\frac{\partial^2 C_S}{\partial y^2} + D_z\frac{\partial^2 C_S}{\partial z^2} - \Theta_S, \tag{4}$$

where $D_y$ and $D_z$ are constant lateral and vertical turbulent diffusivities (streamwise turbulent flux is assumed to be negligible compared with the mean advective flux). The removal of virgin egg and sperm by successful fertilization is given by $\Theta_E$ (Equation 1) and $\Theta_S$ (Equation 2), respectively; these reaction terms couple the two transport equations. The egg and sperm are assumed to be released at separate locations at constant rates $Q_E$ and $Q_S$, respectively. Under these conditions, the resulting mean distributions of gametes have analytical steady-state solutions only in the limiting case where the effect of gamete removal by fertilization on the concentration of virgin gametes is negligible, thus decoupling Equations 3 and 4. In this case, the mean gamete distributions $\overline{C_E}$ and $\overline{C_S}$ can be found using diffusion theory (Csanady 1973), with the resulting plumes described by

$$\overline{C_E}(x, y, z) = \frac{Q_E}{4\pi x\sqrt{D_y D_z}} \left\{ \exp\left[ -\frac{y^2}{4D_y x/U} - \frac{(z-h)^2}{4D_z x/U} \right] + \exp\left[ -\frac{y^2}{4D_y x/U} - \frac{(z+h)^2}{4D_z x/U} \right] \right\} \quad (5)$$

and

$$\overline{C_S}(x, y, z) = \frac{Q_S}{4\pi x\sqrt{D_y D_z}} \left\{ \exp\left[ -\frac{y^2}{4D_y x/U} - \frac{(z-h)^2}{4D_z x/U} \right] + \exp\left[ -\frac{y^2}{4D_y x/U} - \frac{(z+h)^2}{4D_z x/U} \right] \right\}, \quad (6)$$

where $h$ is the height above the bed at which the gametes are released. In each plume equation, $x$ and $y$ are measured from the respective egg or sperm release location. The lateral gamete distributions are Gaussian, with standard deviation

$$\sigma_y = \sqrt{2D_y x/U}\,. \quad (7)$$

The vertical distributions are modified by the presence of the no-flux constraint at the bed $z = 0$.

**Figure 1*a*** shows the typical distributions of mean gamete concentrations in a horizontal plane above the bed calculated using Equations 5 and 6; **Figure 1*b*** shows the spatial distribution of the mean fertilization rate calculated as the product of the mean gamete concentrations. The fertilization rate peaks a short distance downstream of the sources, and then decays toward zero downstream owing to dilution of the mean gamete concentration fields.

Denny & Shibata (1989) pioneered the use of an effective turbulent diffusivity to estimate mean gamete distributions and resulting fertilization rates, using the sea urchin *Strongylocentrotus purpuratus* as a test species. Their work was the first to highlight the potential inefficiency of broadcast spawning as a reproductive strategy owing to the deleterious effects of mean turbulent dilution. The approach was later used to compare predicted gamete concentrations and fertilization rates with field measurements for the spawning sea stars *Acanthaster planci* (Babcock et al. 1994) and *Oreaster reticulatus* (Metaxas et al. 2002). Variations on the theme have also been used to study the effects of adult spatial distribution and population structure (Levitan & Young 1995, Claereboudt 1999, Lauzon-Guay & Scheibling 2007).

Mean gamete distributions obtained in this manner may provide reasonable estimates of the time-average concentrations of egg and sperm and downstream locations, as long as the effective diffusivities are chosen appropriately. But the main value in this approach is simply its convenience: Very little detailed information is required about properties of the flow and the gametes. However, the assumption that gametes disperse as passive scalars is unlikely to be particularly accurate, given the complex physical properties of the gametes (Thomas 1994a,b). More critically, use of mean gamete distributions to calculate fertilization rates is likely to be inappropriate in many flow scenarios.

## 4. THE PARADOX OF TURBULENT MIXING

A fundamental paradigm of turbulent stirring and mixing is that turbulence leads to efficient dilution of transported scalars. Initially, turbulence stretches a scalar blob into elongated filaments.

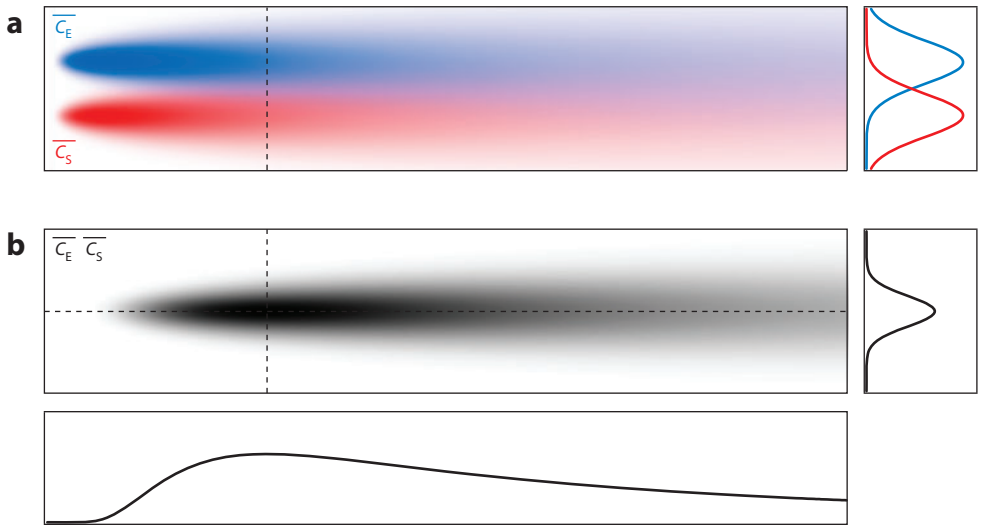


**Figure 1**

Typical mean gamete and fertilization rate distributions in a horizontal plane above the bed, with flow from left to right. (*a*) Mean egg (*blue*) and sperm (*red*) concentrations calculated using Equations 5 and 6 for bed-level sources at the left edge of the plot. The smaller plot to the right shows transverse profiles of egg and sperm at the location indicated by the dashed line. (*b*) Spatial distribution of the mean fertilization rate calculated as the product of the mean gamete concentrations (Equation 1). The plots to the right and below show transverse and streamwise profiles of fertilization rate, respectively, at the locations indicated by the dashed lines.

Stretching increases the interfacial area between the scalar and the surrounding fluid, sharpens the scalar gradients across these interfaces, and leads to enhanced diffusion across the interface, resulting in the dilution of the scalar. The end result is that introduced scalar concentrations are mixed into a uniformly dilute solution. Turbulent dilution of gametes is deleterious to efficient fertilization, because dilute egg and sperm concentrations cannot produce large fertilization rates in the fertilization kinetics relationship.

This leads to a paradox in broadcast spawning. Gametes are typically released by adults into turbulent flow environments, and if turbulence sufficiently dilutes the gamete concentrations, the resulting fertilization rates are very small. The work by Denny & Shibata (1989) exemplifies this paradox: No reasonable parameters in their model lead to predictions of fertilization rates that match those measured in the field. If turbulent dilution is ruinous to broadcast spawning, then how does the process succeed for a range of species living in turbulent environments? Are there other physical aspects of fluid stirring that might mitigate the effects of dilution? Have benthic organisms evolved to take advantage of these subtleties, such that efficient fertilization can take place before irreversible dilution sets in?

The remainder of this review is devoted to exploring reasons that the mean gamete distribution model used by Denny & Shibata (1989) might dramatically underpredict fertilization rates. The primary reason is likely that the model does not (and cannot) include the instantaneous effects of fluid stirring, which are quite complicated. Instantaneous turbulent processes produce complex, filamentous spatial distributions of transported gametes. The local mean concentration of the gametes is the average of a wide range of instantaneous concentrations that pass that point. Thus, even though the mean gamete concentration is predicted to be small owing to turbulent dilution, the instantaneous concentrations within filaments may be much higher, with significantly less

dilution. Furthermore, a range of physical processes may cause such high-concentration filaments of egg and sperm to aggregate in an instantaneous sense, producing episodic events of intense fertilization. These ideas are reviewed in Section 5.

At a much smaller scale, chemoattractant plumes released by benthic eggs are stirred and stretched by the local flow, and motile sperm utilize chemotaxis to actively search for eggs. Thus, at least at small scales, sperm certainly do not behave like passive scalars. The roles of chemoattractant plumes, sperm motility, and sperm taxis and their potential ability to enhance fertilization rates are reviewed in Section 6.

## 5. LARGE SCALE: THE EFFECT OF FLOW ON GAMETE AGGREGATION

### 5.1. Mean Versus Instantaneous Structure

Turbulent flows stretch and stir scalars into complex patterns as they are transported downstream. The complexity in the scalar distribution results from an integrated exposure to complexity in the turbulent velocity field. Although it may be convenient to average this complexity into a mean distribution, structural details that may be important to the problem are then lost. In the case of chemical reactions between two scalars, details of the instantaneous scalar distributions are critical to predicting the resulting reactions (Crimaldi et al. 2006, 2008). Likewise, in the case of broadcast spawning, details of the instantaneous gamete distributions may be critical to the resulting fertilization rate (Crimaldi & Browning 2004).

The structure of plumes of passive scalars in benthic boundary-layer flows has been studied extensively in laboratory flumes (Crimaldi & Koseff 2001, Crimaldi et al. 2002, Webster et al. 2003, Crimaldi & Koseff 2006). In these studies, the scalar is a fluorescent dye, and planar laser-induced fluorescence (PLIF) (reviewed in Crimaldi 2008) is used to quantify the instantaneous scalar distribution at various locations downstream. Time histories of these measurements can be averaged to determine the mean scalar distribution, enabling a comparison of the mean and instantaneous structures.

**Figure 2** shows false-color images of scalar concentrations of a single passive scalar plume measured using PLIF in a laboratory flow. It is clear that the mean profile is not a good predictor of instantaneous concentrations, and that localized filaments in the instantaneous structure can have concentrations that greatly exceed the dilute concentrations in the mean distribution.

### 5.2. The Role of Instantaneous Structure in Fertilization

Clearly, instantaneous distributions of scalars in turbulent plumes can have dramatically different structural qualities compared with their mean descriptions. We now turn to why the mean (time-average) fertilization rate may not be well predicted by mean gamete distributions, and may instead depend on knowledge of the instantaneous distributions. To this end, we employ a standard technique called the Reynolds decomposition to decompose each local gamete concentration into the sum of a mean and a fluctuating component. Thus, the egg concentration can be decomposed as

$$C_E(t) = \overline{C_E} + c'_E(t), \tag{8}$$

where $C_E(t)$ is the instantaneous, time-varying local concentration; $\overline{C_E}$ is the mean concentration; and $c'_E(t)$ is the fluctuating component relative to the mean. Likewise, the sperm concentration can be decomposed as

$$C_S(t) = \overline{C_S} + c'_S(t). \tag{9}$$

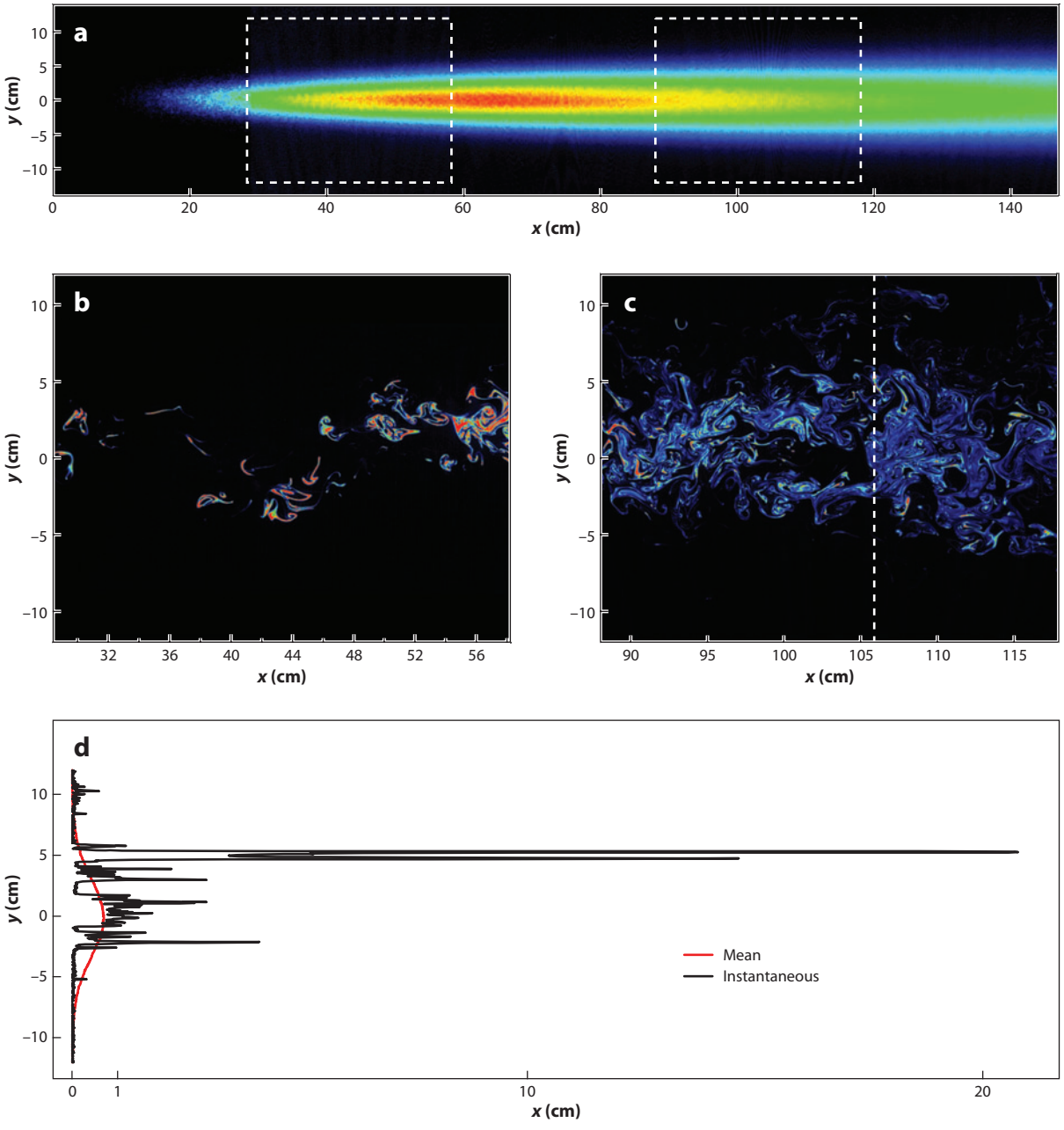


**Figure 2**

Laboratory measurements of mean and instantaneous scalar concentrations using planar laser-induced fluorescence. The scalar source was located flush with the bed at ($x = 0, y = 0$); the images were taken in a horizontal plane 2 cm above the bed (for details, see Crimaldi et al. 2002). (*a*) Mean plume concentrations averaged from 8,000 instantaneous images. (*b*,*c*) Single instantaneous concentration distributions corresponding to the locations indicated by the two dashed rectangles in panel *a*. The colors are modified so that they correspond to concentrations that are 10 times those shown in panel *a*. (*d*) Comparison of mean and instantaneous lateral profiles at $x = 106$ cm, indicated by the dashed line in panel *c*. The concentration profiles are scaled by the maximum mean concentration in panel *a*. Adapted from Crimaldi et al. (2002) and Crimaldi & Browning (2004).

Rewriting the fertilization kinetics model $\Theta_E = \Phi C_E C_S$ (Equation 1) in terms of the concentration decompositions and then time averaging the result yields four terms, two of which are nonzero (Crimaldi et al. 2006):

$$\overline{\Theta_E} = \overline{\Phi C_E C_S} = \Phi \left( \overline{C_E}\,\overline{C_S} + \overline{c'_E c'_S} \right). \tag{10}$$

Thus, the mean fertilization rate depends on the sum of two quantities. The first, $\overline{C_E}\,\overline{C_S}$, is simply the product of the mean distributions of egg and sperm. The second, $\overline{c'_E c'_S}$, is the covariance of the instantaneous egg and sperm concentration distributions. The covariance is a measure of spatial correlations between the two distributions. If the covariance term is zero or small compared with $\overline{C_E}\,\overline{C_S}$, then using the product of the mean gamete distributions is a reasonable approach for estimating the mean fertilization rate. However, if the covariance term is large, then using the product of the means can yield spectacularly inaccurate results. As discussed in Section 3, fertilization predictions by Denny & Shibata (1989) and other similar studies relied solely on the product of the mean distributions. Crimaldi & Browning (2004) suggested that the underprediction of measured fertilization rates by these models is due to the lack of inclusion of the covariance term that accounts for spatial correlations between the instantaneous distributions of egg and sperm.

The relative importance of the covariance term relative to the product of the means can be quantified with a ratio called the segregation parameter (Danckwerts 1952, Hill 1976):

$$\alpha = \overline{c'_E c'_S} \Big/ \left( \overline{C_E}\,\overline{C_S} \right). \tag{11}$$

Using this definition, we can express the time-average fertilization rate from Equation 10 in terms of the mean gamete distributions as

$$\overline{\Theta_E} = (1 + \alpha)\Phi\,\overline{C_E}\,\overline{C_S}, \tag{12}$$

which highlights the amplifying effect of a nonzero $\alpha$ value on resulting fertilization rates. Both physical and biological processes might produce spatial correlations between egg and sperm distributions, leading to nonzero covariance terms and nonzero values of $\alpha$. In Section 5.3, we review macroscopic flow-based processes that can lead to localized aggregation of gametes, enhancing fertilization rates. In Section 6, we discuss small-scale biological processes related to chemical signaling and sperm taxis that can produce aggregation at the gamete scale.

### 5.3. Large-Scale Aggregation Processes

Fertilization is analogous to a transport and reaction process between two reactants, which in this case are the egg and sperm (Equations 3 and 4). The reaction is complicated by the biological constraint that the egg and sperm are initially released from different locations and by the fact that they are separated by a third, nonreactive scalar (gamete-free water). Most studies of the effect of structured stirring and turbulence on reactions consider a simpler scenario: The two reactants are not initially distant but instead share a material interface (they are initially separate but not distant). In the simpler scenario, it is well known that fluid stirring enhances mixing between the two reactants and thus enhances reaction rates (e.g., Hill 1976). However, if the two scalars are initially separated by some distance, as they are in broadcast spawning, then the role of fluid stirring in subsequent reactions is more complicated and not well understood. For turbulence to enhance the reaction rate, the flow must somehow locally aggregate the two scalars without first diluting them to the point that the resulting reaction rate would be insignificant.

Although fluid stirring is most generally associated with dispersion, mixing, and dilution of introduced scalars, a number of flow-related mechanisms can at least temporarily produce local aggregation of transported solutes or particles. That is, the very flow mechanisms that produce

efficient dilution at sufficiently long timescales can, at intermediate timescales along the way, do what amounts to the exact opposite of dilution. These mechanisms could promote local coalescence of gametes, enabling dramatic local enhancement in fertilization rates at intermediate timescales even though the ultimate fate of the gametes is to be dispersed and diluted.

**5.3.1. Passive aggregation.** The most fundamental aggregation processes are associated with the physics of the flow alone and do not depend on any special features of the gametes (such as the size and inertia of the gametes, the viscosity and rheology of the gamete matrix, and gamete motility). These flow processes can produce local (albeit temporary) aggregation of even purely passive scalars like solutes or dyes. In the case of a single scalar, local folding of the filaments can lead to local aggregation of same-scalar filaments at intermediate timescales, resulting in additive rather than dilution-like behavior (Villermaux & Duplat 2003). Until recently, the role and even existence of turbulent processes that aggregate two initially distant scalars relevant to the broadcast-spawning process were completely unstudied. However, a series of recent investigations have begun to demonstrate that these processes do indeed exist in structured flows, and a hierarchical approach has considered the effects in a single vortex, in vortex-dominated obstacle wakes, and in full three-dimensional turbulence. Each of these is reviewed in turn below.

One of the simplest structured flow fields is that of a single two-dimensional vortex. A vortex is a good model system in that it provides insight into more complex flows that consist of multiple interacting vortices. For example, laminar wakes behind obstacles consist of a sequence of vortices shed periodically from either side of the obstacle, and turbulent flows consist of a continuous range of vortices (often termed eddies in that context) that interact in a chaotic manner. The flow from a single vortex has an analytical description that facilitates analytical modeling (e.g., Meunier & Villermaux 2003). In a pair of studies, Crimaldi et al. (2006, 2008) investigated the effect of stirring by a single vortex on reactions between two initially distant scalars (see **Figure 3**). The vortex flows in circles about its center, with a velocity that decays inversely with radius. The velocity gradient strains the parcels into long, thin filaments, enhancing scalar gradients and diffusion in the radial direction. The scalar fields quickly assume a spiral geometry associated with the flow, become correlated with each other, and begin to overlap. As scalar concentrations coalesce, reaction rates

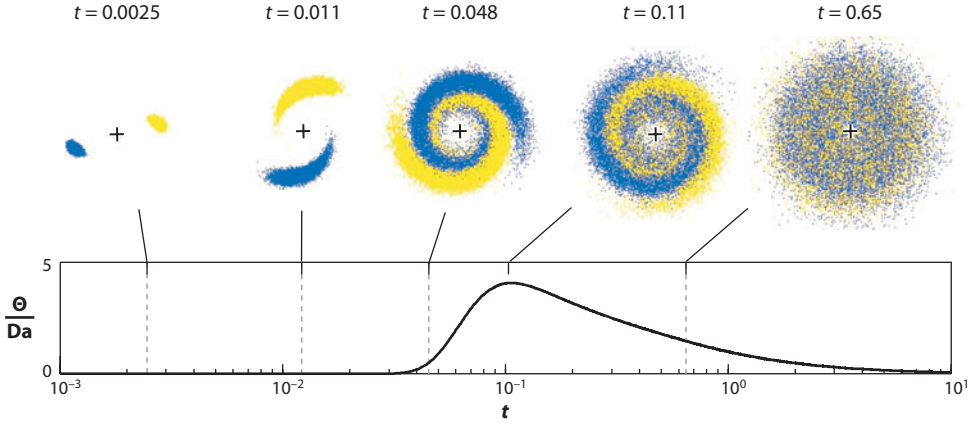


**Figure 3**

Distribution and subsequent reaction of two initially distant scalars (*blue* and *yellow parcels*) in a single ideal vortex. The vortex flows counterclockwise, with circular streamlines centered on the plus symbols. Adapted from Crimaldi et al. (2008).

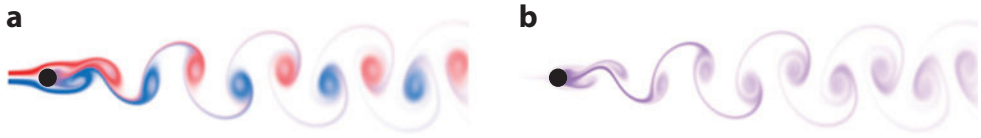


**Figure 4**

Stirring and mixing of passive reactive scalars in the unsteady wake of a round obstruction. (*a*) A typical instantaneous distribution of the two scalar concentrations (*red* and *blue*). (*b*) The corresponding reaction rate formed as the product of the two concentrations. Without the wake, the reaction would be diffusion limited and negligible by comparison. Adapted from Crimaldi & Kawakami (2013).

grow rapidly until they reach a peak. Beyond that time, radial diffusion begins to break down the flow-induced filament structure, and the resulting dilution leads to lowered reaction rates. Note that, in the absence of the vortex field, diffusion alone would have to bridge the large distance separating the scalars, leading to dramatically lower reaction rates.

Given that single vortices can aggregate initially distant scalars and enhance reactions, Crimaldi & Kawakami (2013) used numerical simulations to investigate a slightly more complicated flow involving interacting vortices shed behind a circular obstruction. The goal was to understand how flow around an obstacle such as a coral head could produce hydrodynamic stirring conditions that are favorable to fertilization success. In the simulations, continuous filaments of two diffusive scalars (see **Figure 4*a***) are released into a laminar flow upstream of an obstruction, separated by some distance perpendicular to the flow direction. Absent the obstruction, reactions are severely limited by the lateral separation of the scalars, because the only mechanism that can bridge the separation is diffusion. However, the simulations showed that the structured wake downstream of the obstruction efficiently aggregates the scalars along filament braids that connect the vortex cores. The reaction rate (**Figure 4*b***) is concentrated in these braids and is dramatically enhanced relative to the obstacle-free flow. In the simulation shown in **Figure 4**, the scalars are separated only by a relatively small distance (one-quarter of the obstacle diameter) and are released symmetrically about the obstacle centerline. However, the study showed that the reaction enhancement is robust for a range of release geometries. Other marine ecology studies at larger scales have shown that fluid wakes behind islands can alter nutrient distributions (Hasegawa et al. 2004) and phytoplankton dynamics (Sandulescu et al. 2007). Thus, structured stirring in obstacle wakes may serve to aggregate initially distant gametes and significantly enhance fertilization rates.

More recent work has demonstrated that much more complicated flows involving three-dimensional turbulence also locally aggregate passive scalars. Soltys & Crimaldi (2011) developed an experimental technique to simultaneously measure the concentrations of two passive scalars released from separate locations in turbulent flows. This technique enables investigators to directly measure instantaneous scalar aggregation and identify processes that produce the aggregation. **Figure 5** shows the spatial distribution of two passive scalars released at different heights in a homogeneous isotropic turbulent flow in a laboratory flume. Even though the scalars are released at separate locations and are completely passive, it is clear that spatial correlations develop between their distributions. **Figure 5*c*** quantifies this effect, showing vertical profiles of the segregation parameter $\alpha$ (Equation 11) for upstream and downstream locations. The results show that $\alpha$ can be significantly different from zero and tends to increase with distance downstream and away from the centerline. At the downstream location, which is still less than 3 m from the source, the value of $\alpha$ has grown to 20 away from the centerline; this indicates that reaction contributions from instantaneous processes are locally 20 times larger than those that would be predicted from the mean distributions alone (Equation 12). Further downstream, the effect is likely even larger. This

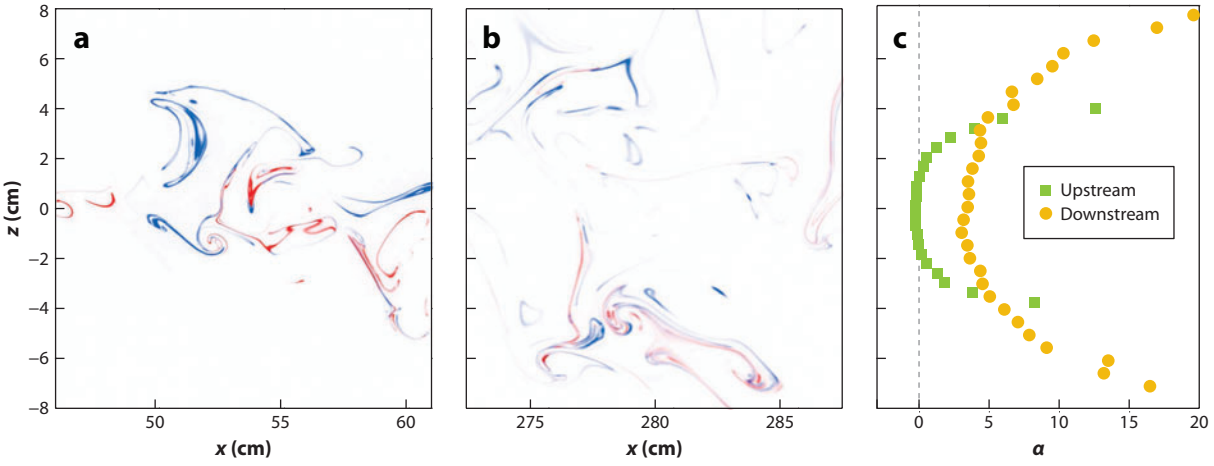


**Figure 5**

Laboratory experiments of two passive scalars (*blue* and *red*) released at different heights ($z = +0.7$ cm for the blue scalar, $z = -0.7$ cm for the red scalar) in a homogeneous isotropic turbulent flow. (*a*,*b*) Representative instantaneous concentration distributions for an upstream location (near $x = 50$ cm; panel *a*) and a downstream location (near $x = 275$ cm; panel *b*). (*c*) Profiles of $\alpha$ (see Equations 11 and 12) for these two cases. Data provided by Michael Soltys.



experimental work provides direct evidence of mechanisms in turbulent flows that might produce fertilization rates dramatically larger than those predicted by studies that consider only the mean distribution of gametes.

Bathymetry and shore topography at spawning sites can also serve to aggregate gametes and limit dilution. Denny et al. (1992) used field experiments and a mathematical model to show that surge channels on wave-swept rocky shores can act as local containment vessels that limit the volume of water available for gamete dilution. The work suggests that 80–100% of eggs in a surge channel might be fertilized if there is a sufficient local male population. Likewise, Pearson & Brawley (1996) demonstrated that gamete sequestration in tide pools can greatly influence fertilization. Females that spawned in tide pools with males present had high fertilization rates, and the study suggested that some species may spawn at low tide to minimize the deleterious effects of dilution.

**5.3.2. Effect of gamete properties on aggregation.** We now turn to flow-related aggregation processes that rely on some physical property of the gametes, such that the gametes are transported differently than passive solutes. First, we consider the effect of gamete size on transport. The fluid mechanics literature is rich in studies of selective aggregation of finite-size particles in fluid flows. Although the studies do not consider gametes per se, it is likely that these processes could play an important role in gamete distributions, particularly for large eggs.

Particles that are sufficiently small and neutrally buoyant move passively with the ambient flow. As particles become larger or nonneutrally buoyant, they respond as if they have inertia relative to the local flow. These inertial effects cause the temporal response characteristics of large or nonneutrally buoyant particles to differ from those of the surrounding fluid (or of dissolved scalars in the fluid). Squires & Eaton (1991) used direct numerical simulations to show that dense particles collect preferentially in regions of low vorticity and high strain rate. Related experiments (Tang et al. 1992, Crowe et al. 1995) showed that particles in intermediate size ranges are focused along the boundaries of coherent vortex structures. Turbulence has been shown to

increase collision rates between inertial particles (Reade & Collins 2000) and to segregate particles with differing densities (Reigada et al. 2001). Even neutrally buoyant particles (of finite size) move in a nonpassive manner owing to particle-flow interactions (Maxey 1990) and aggregate near vortex cores (Babiano et al. 2000). Enhancement of particle encounter rates by turbulence has been demonstrated in the laboratory for synthetic particles (Hill et al. 1992) and with modeling approaches for plankton or other marine particles (Rothschild & Osborn 1988, Squires & Yamazaki 1995, Lewis 2003). Coagulation of finite-size particles is an important mechanism for mass transport in the ocean (reviewed in Jackson & Burd 1998) and in benthic boundary layers (Hill & Nowell 1995, Hill & McCave 2001). Nonetheless, neutrally buoyant particles that are sufficiently small are often assumed to move passively, without disturbing the ambient flow. In this case, the turbulent particle advection problem can be approximated by using dissolved passive scalars (e.g., fluorescent dye) as surrogates for the particles. This is convenient, because there is a large body of literature on the turbulent mixing of passive scalars (reviewed in Warhaft 2000).

Gamete buoyancy varies between species, influences gamete distribution within the water column, and may increase the chances of intraspecific egg and sperm contact (Thomas 1994b). This effect is likely to be most pronounced for floating gametes. At the simplest level, gamete dilution may be suppressed on the two-dimensional plane of the free surface relative to the three-dimensional space of the water column (Oliver & Willis 1987). A numerical model (Moláček et al. 2011) compared encounter rates for buoyant and nonbuoyant gametes and demonstrated that the fertilization advantage for floating gametes is robust and significant, even when costs associated with traveling to the surface are considered.

On a more complex level, this advantage may be further enhanced owing to physical differences in the way floating particles are stirred relative to submerged particles. Buoyant gametes follow path lines on the free surface of the turbulent flow in which they are released. The transport and coalescence of floating particles are fundamentally different from subsurface transport owing to differences in the nature of free-surface turbulence. The kinematic boundary condition at the free surface (vertical velocities = 0) produces a blockage layer that increases horizontal turbulence intensities at the expense of those in the vertical direction; the dynamic boundary condition at the surface (stress = 0) results in a thinner surface layer characterized by fast variations of the horizontal vorticity components (Shen et al. 1999). The surface flow (and the paths of particles following it) is compressible (meaning that particles can aggregate) even when the underlying flow is incompressible. This results in regions of surface flow convergence (corresponding to downwelling in the bulk flow) and divergence (corresponding to upwelling) (Kumar et al. 1998). The inability of floating particles to enter the bulk flow in surface convergence zones therefore leads to coalescence. The extent to which the surface flow deviates from incompressibility is quantified by the compressibility coefficient

$$C = \overline{(\nabla_s \cdot \mathbf{u}_s)^2} / \overline{(\nabla_s \mathbf{u}_s)^2}, \tag{13}$$

where the "s" subscript denotes that only derivatives and velocities in the surface plane are computed. This quantity has been found to be close to 1/2, both experimentally (Goldburg et al. 2001) and numerically (Eckhardt & Schumacher 2001).

Floating particles cluster owing to the effects of turbulence (Eckhardt & Schumacher 2001; Schumacher & Eckhardt 2002; Boffetta et al. 2004, 2006; Cressman et al. 2004; Bandi et al. 2008; Ducasse & Pumir 2008), surface waves (Denissenko et al. 2006, Lukaschuk et al. 2006), surface tension (Singh & Joseph 2005), or wind-induced Langmuir circulations (Larson 1992, Thorpe 2004). Nonetheless, the quantitative effect of these free-surface aggregation mechanisms on gamete distribution and fertilization success is unknown.

Broadcast spawners typically release gametes that are packaged in a mucous matrix. The rheology of the matrix is typically different from that of the ambient fluid, which alters the way the gametes are dispersed and diluted by the flow. The matrix is often highly viscous, which may act to minimize dilution (Thomas 1994b, Marshall 2002). The viscous quality also lends a certain stickiness to the gametes, enabling them to adhere to the substratum or to adults (Picken & Allan 1983, McEuen 1988, Svane & Havenhand 1993, Thomas 1994a, Yund & Meidel 2003), where they may be preferentially fertilized. The matrix rheology is typically non-Newtonian and exhibits shear-thinning properties that facilitate extrusion through the gonoduct (Thomas 1994a). Shear-thinning fluids disperse and mix differently than Newtonian fluids (e.g., Niederkorn & Ottino 1994), but the overall role of viscosity and rheology in gamete distribution and fertilization success is unknown.

## 6. SMALL SCALE: THE ROLES OF CHEMOATTRACTANT PLUMES, SPERM MOTILITY, AND SPERM TAXIS

Turbulent energy in large eddies cascades down to smaller and smaller eddies until viscous action impedes the process and mechanical energy is viscously dissipated to heat. The Kolmogorov microscale $\eta$ is a measure of the size of the smallest eddies in a given flow; it is set by the kinematic viscosity $\nu$ and the amount of energy being transferred down the cascade, which, in equilibrium, is equal to the rate of turbulent energy dissipation $\varepsilon$. In coastal environments, the magnitude of $\varepsilon$ ranges from $10^{-3}$ to $10^{0}$ cm$^2$ s$^{-3}$ (Kiørboe & Saiz 1995, Karp-Boss et al. 1996). The magnitude of $\eta$, given by

$$\eta = \left(\frac{\nu^3}{\varepsilon}\right)^{1/4}, \tag{14}$$

is typically on the order of 1 mm in turbulent benthic habitats (Lazier & Mann 1989). Individual gametes, which are smaller than $\eta$, therefore experience a very different set of physical conditions than clouds of gametes at the centimeter or meter scale do. Below the Kolmogorov scale, gametes are influenced largely by the single dissipative vortex in which they currently reside, which imposes an unsteady but slowly varying linear shear (Lazier & Mann 1989, Karp-Boss et al. 1996, Jumars et al. 2009). At these scales, the roles of chemoattractant release, sperm motility, and sperm taxis can enhance gamete encounter rates and affect fertilization success.

At the simplest level, sperm motility acts to disperse a localized concentration of sperm. Because gametes are large compared with the molecular scale, they do not experience significant Brownian motion or diffusion, as solutes do. But sperm motility acts as a macroscopic analog to molecular diffusion and causes sperm to disperse in a way that is mathematically similar to diffusion (Inamdar et al. 2007). Observing this dispersion in anything resembling a realistic flow is beyond the scope of current methods.

A model that explicitly predicts gamete encounter rates from sperm motility and fluid motion is sorely lacking. The physical basis for such a model may be borrowed from oceanography (Gerritsen & Strickler 1977, Rothschild & Osborn 1988, Kiørboe & Saiz 1995, Visser & Kiørboe 2006). Simple rules of thumb have been used quite successfully to describe the effects of flow (turbulence) and cell/animal locomotion on predator-prey encounters among tiny zooplankton. To first order, predictions should be similar for cells and organisms of similar sizes, shapes, and motilities. Here, we limit discussion to spatial scales over which eggs and sperm are at least two to three times smaller than $\eta$. Admittedly, some rocky intertidal species (such as honeycomb worms, sea urchins, and limpets) broadcast their gametes under extreme hydrodynamic conditions of crashing waves, where length scales of the tiniest eddies may be smaller than egg diameters (Lewis 1986,

Barry 1989, Denny & Shibata 1989, Denny et al. 2002). For these select species and habitats, fertilization undoubtedly occurs via gamete encounters that are dominated by physical transport.

To fully appreciate the ecological context for fertilization requires understanding the relationship between flow and cell motility. Where and when does sperm behavior make a difference? Based on a time-tested model for tiny zooplankton (scales $\ll \eta$) (Kiørboe & Saiz 1995), sperm-egg encounter rate ($E$) depends on male ($C_S$) and female ($C_E$) gamete concentrations (number of individuals per unit of fluid volume) and on components of sperm behavior ($\beta_{behavior}$) and fluid motion ($\beta_{flow}$):

$$E = (\beta_{behavior} + \beta_{flow}) C_E C_S. \quad (15)$$

A simple conceptual example now represents the behavioral component. Let us assume that sperm swim with a defined perceptive distance ($r_S$) and speed ($u_S$) along a straight path while searching for a nonmotile, spherical egg of radius $r_E$. The rate of fluid volume scanned by an individual male gamete can be described as

$$\beta_{behavior} = \pi (r_E + r_S)^2 u_S. \quad (16)$$

Sperm swim naturally in three-dimensional helices with translational (straight-ahead) and rotational (side-to-side) components (Crenshaw 1996). Swimming speed is defined as the forward (translational) velocity component, and perceptive distance is taken as the radius or pitch in the helical path. These properties agree well with those applied previously in studies on zooplankton (Kiørboe & Saiz 1995, Visser & Kiørboe 2006, Maldonado & Latz 2011). Red abalone gametes are used below for illustration; more is known about the interactions between small-scale fluid dynamics, chemotaxis, and fertilization in red abalone than in any other species. When sperm search for mates at low shears, empirical mean values are 43 $\mu m\ s^{-1}$ for swimming speed, 24 $\mu m$ for pitch, and 113 $\mu m$ for egg radius (Riffell & Zimmer 2007, Zimmer & Riffell 2011). Employing Equation 16, we find that $\beta_{behavior} = 2.5 \times 10^{-3} mm^3\ s^{-1}$.

In flow, at sub-Kolmogorov scales, male and female gametes are passively transported at different speeds because of fluid shear. Consequently, sperm need not swim (though they often do) to move toward an egg. The volume flow rate scanned by a male gamete even in the absence of motility is (Kiørboe & Saiz 1995)

$$\beta_{flow} = 0.42\pi (\varepsilon/\nu)^{1/2} (r_E + r_S)^3, \quad (17)$$

where $\nu$ is kinematic viscosity and $\varepsilon$ is turbulent energy dissipation rate. The term $(\varepsilon/\nu)^{1/2}$ is an estimate of the magnitude of shear imposed by fluid stirring on gamete transport processes. When $\beta_{flow} > \beta_{behavior}$, fluid stirring dominates sperm motility and controls male-female gamete contact rates. Equating Equations 16 and 17, we can solve for the critical turbulent energy dissipation rate ($\varepsilon_{crit}$) at which flow and sperm motility effects are matched:

$$\varepsilon_{crit} = 5.7 \left( \frac{\nu\, u_S}{r_E + r_S} \right)^2. \quad (18)$$

This variable $\varepsilon_{crit}$ can be viewed as a type of threshold, delineating when sperm behavior matters as opposed to when it is overwhelmed by the strength of fluid stirring and shear. For red abalone, $\varepsilon_{crit} = 6.7 \times 10^{-3}\ cm^2\ s^{-3}$. In comparison, field flow measurements in native red abalone spawning habitats yield $\varepsilon$ values ranging from $9.2 \times 10^{-4}\ cm^2\ s^{-3}$ (10th percentile) to $5.8 \times 10^{-2}\ cm^2\ s^{-3}$ (90th percentile) (Riffell & Zimmer 2007). Thus, sperm behavior likely does matter under select natural conditions and may contribute significantly to fertilization success.

These scaling arguments can provide important insights, but they are at best first-order approximations. Because of serious technology limitations, field tests cannot isolate behavioral effects from flow effects. Direct numerical simulations and laboratory experiments using simplified

flow abstractions thus provide the most powerful tools to continue investigation. Theoretical and empirical approaches can work hand in hand, setting boundary conditions to minimize the number of experimental treatments while providing more realism to computational explorations. For red abalone eggs and sperm, individual encounters between male and female gametes were imaged directly in laboratory-generated, steady (one-dimensional), laminar shear flows (Zimmer & Riffell 2011). The results were consistent with model predictions even though the experiments lacked some critical properties of ocean environments (e.g., fluctuating terms of velocity and vorticity) (Jumars et al. 2009). As determined empirically, sperm motility and chemotaxis were highly effective at promoting fertilization when turbulent energy dissipation rates ranged from $1 \times 10^{-4}\,\mathrm{cm^2\,s^{-3}}$ to $2.5 \times 10^{-3}\,\mathrm{cm^2\,s^{-3}}$, mildly effective when these rates ranged from $1 \times 10^{-2}\,\mathrm{cm^2\,s^{-3}}$ to $4 \times 10^{-2}\,\mathrm{cm^2\,s^{-3}}$, and ineffective in more strenuous flows. These findings all identify sperm behavior and flow as cogent partners for sex in the sea.

The encounter rate model used above (Kiørboe & Saiz 1995) has many strengths and some weaknesses. Among its strengths are the relative ease with which it can be applied to a vast number of biological systems and, in many cases, its excellent description of particle-particle (or organism-organism) interactions. Yet this model assumes independence between the $\beta_{\mathrm{behavior}}$ and $\beta_{\mathrm{flow}}$ terms—i.e., no effect of flow on behavior. Recent experiments have shown significant effects of flow on egg and sperm behavior and on egg-derived chemoattractant plumes. Consequently, observations for male-female gamete encounters deviate from those predicted, especially at higher shears.

Shear causes suspended particles to rotate. When transported passively, spherical eggs spin at a constant rate, whereas swimming sperm (as prolate spheroids) align with flow streamlines at higher shears and flip (or rotate) periodically (Bartok & Mason 1957, Karp-Boss & Jumars 1998). Gamete rotation rates for red abalone gametes have been measured and compared with theoretical predictions for spheres (eggs) and prolate spheroids (sperm) within one-dimensional laminar shear flows (Jeffery 1922):

$$0.5T = 2\pi(\nu/\varepsilon)^{1/2}\left(r_{\mathrm{G}} + \frac{1}{r_{\mathrm{G}}}\right), \tag{19}$$

where $r_{\mathrm{G}}$ is the axis ratio (length/width) of a gamete (e.g., $r_{\mathrm{G}} = 1$ for the egg) and $T$ is the period of gamete rotation. For eggs, measurements and predictions were in excellent agreement at all shears tested (Riffell & Zimmer 2007). As shear increased, female gametes rotated continuously and with faster instantaneous velocities. The behavior of dead sperm also conformed to the theoretical model under all conditions. Although live sperm did not tumble at lower shears, they began to rotate, much like dead cells, at turbulent energy dissipation rates $\varepsilon > 1.6 \times 10^{-1}\,\mathrm{cm^2\,s^{-3}}$. The transition in active sperm behavior to that of being passively transported and rotated was predicted based on the ratio between the propulsive force during steady swimming

$$F_{\mathrm{swim}} = \mu\left(\frac{4\pi l}{\ln(2l/d) - \frac{1}{2}}\right)u_{\mathrm{S}} \tag{20}$$

and the shear force acting on the cell

$$F_{\mathrm{shear}} = c\mu\frac{\partial u}{\partial y}. \tag{21}$$

Here, $\mu$ is the dynamic viscosity of seawater, $l$ is the length of the sperm body (excluding the flagellum), $d$ is the width of the cell, $u_{\mathrm{S}}$ is the swimming speed, $c$ is the average surface area of a sperm, and $\partial u/\partial y$ is shear due to the velocity gradient. At $\varepsilon = 1.6 \times 10^{-1}\,\mathrm{cm^2\,s^{-3}}$, forces generated by swimming cells and by shear were equally matched ($F_{\mathrm{swim}}/F_{\mathrm{shear}} = 1$).

In experiments in a Taylor-Couette flow tank, egg rotation inhibited sperm contact and hence fertilization (Riffell & Zimmer 2007). As flow approached a rotating egg, the fluid accelerated,

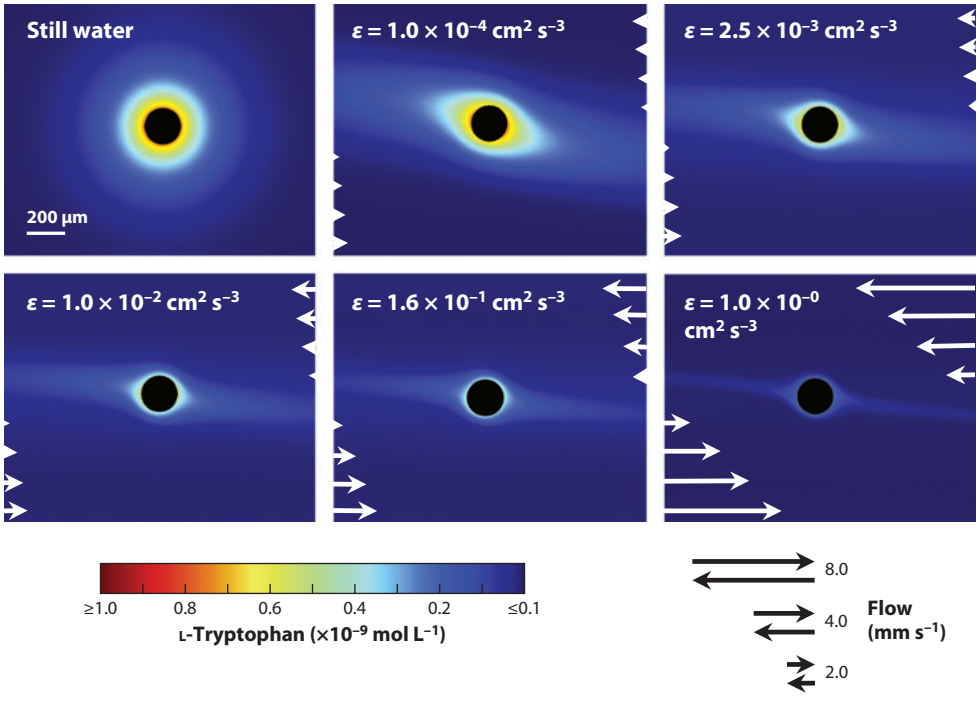


**Figure 6**

Theoretical concentration distributions of the chemoattractant L-tryptophan surrounding red abalone eggs (*black circles*) in still water and in one-dimensional, laminar shear flows (with $\varepsilon$ denoted in units of $cm^2\ s^{-3}$). Each plot is a two-dimensional slice cut through the center of an egg. White arrows denote flow velocity vectors (speeds and directions). The *x* axis is parallel to the direction of flow; the *y* axis is orthogonal to the direction of flow and parallel to the direction of shear. Tryptophan plumes were produced through three-dimensional numerical simulations that used a coupled convection-diffusion model, taking into account egg rotation rate at each shear and assuming a constant and continuous tryptophan release over the entire egg surface for 4 min. Model parameters (flow speed and direction, fluid shear, attractant release rate and diffusion coefficient, egg diameter and rotational velocity, and water temperature) accurately portrayed conditions in experiments on sperm swimming behavior and chemotaxis (see **Figure 7**). Adapted from Zimmer & Riffell (2011).

the streamlines compressed or closed, and the shear stress increased locally near the surface. Consequently, the likelihood of sperm slipping around the egg surface, rather than encountering it, also rose significantly with egg rotation rate. The results were consistent and showed the profound effects of flow-induced gamete rotation on sperm-egg interactions.

Eggs release chemoattractants that serve as navigational cues for sperm at the gamete scale. To investigate the role of local flow in chemoattractant concentration distributions, Zimmer & Riffell (2011) numerically modeled chemoattractant plumes surrounding individual eggs in still water and over a range of steady, one-dimensional, laminar shears. Eggs were allowed to freely rotate owing to the action of the local velocity gradient; this rotation locally thinned the boundary layer and increased shear stress near the egg surface. A constant flux of the chemoattractant L-tryptophan was released over the entire egg surface.

From modeling results (**Figure 6**), cross-sectional areas and volumes of egg-derived tryptophan plumes were predicted to peak in still water (i.e., diffusion alone) and in weak shears and to decrease thereafter. Weak shears and slow flows resulted in elevated concentrations that decreased

with increasing distance from an egg. The plumes ultimately expanded along the principal flow axis relative to still water. In contrast, strong shears and fast flows rapidly reduced tryptophan concentrations below the sperm behavioral threshold ($3 \times 10^{-10}$ mol $L^{-1}$, as determined empirically) in all but a very tiny region near the eggs.

The results of empirical experiments using live eggs and sperm strongly supported the theoretical predictions and validated the numerical model of tryptophan plume dynamics (Zimmer & Riffell 2011). In steady, one-dimensional, laminar shear flows, red abalone sperm swam more quickly and navigated directly toward egg surfaces within the predicted egg-derived plumes (**Figure 7**). Sperm located outside the predicted plumes, in contrast, swam more slowly and did not orient significantly with respect to an egg. Shear exerted a strong modulating effect on sperm behavior. Swimming speed and orientation toward an egg peaked at the weakest shears tested and then decayed as shear strengthened. At high shears, flow-generated torques increasingly overwhelmed sperm behavior. These higher shears prevented gametes from swimming actively across streamlines. Sperm aligned parallel to streamlines and cells tumbled at frequencies predicted by theory for passively transported particles. Whereas weak shears promoted sperm locomotory performance and enhanced the attractant plume of egg-derived chemical signals, strong shears inhibited performance and suppressed the plume.

What is unknown is how these chemoattractant plumes are stirred and distorted by unsteady shear whose magnitude and direction vary in Kolmogorov-scale turbulence. The complexity of the instantaneous chemoattractant plumes is likely to be loosely analogous to the high level of complexity seen in large-scale instantaneous plumes (e.g., **Figure 2*b*,*c***), but the physics of the stirring at small scales is clearly different. Also unknown is how the efficacy of sperm chemotaxis is affected by local complexity in the chemoattractant plumes. Studies of these issues will likely be limited to numerical simulations owing to the difficulty of observing these phenomena under realistic flow conditions.

## 7. A HOLISTIC PARADIGM FOR FERTILIZATION ACROSS A RANGE OF SCALES

Benthic invertebrate eggs and sperm face a daunting task as they seek a seemingly chance encounter with one another in a vast turbulent sea. A variety of factors exacerbate the challenge of a successful fertilization event. Eggs and sperm may be initially separated by distances that are huge compared with the sizes of the gametes. Turbulent dispersion threatens to dilute the concentration of gametes, turning the search for an egg into a needle-in-a-haystack problem. Even if fluid motion happens to stir filaments of eggs and sperm into close proximity, the gametes lack the diffusive behavior of solutes that promotes cross-streamline mixing in traditional reactive systems. The process seems destined to fail. Yet broadcast spawning is clearly a viable, successful, and efficient reproductive mechanism used by a range of benthic invertebrates across a range of flow environments. Although the exact reasons for the success are still not clearly understood, we synthesize here a holistic paradigm that provides a simple conceptual framework for understanding how physics and biology conspire over a range of physical scales to overcome long odds and create an efficient system.

The separation between spawning adults is on the order of centimeters or meters, which is at least several orders of magnitude larger than an egg. Given that sperm swimming speeds are in the range of 0.05–0.3 mm $s^{-1}$ (Gray 1955, Levitan et al. 1991, Levitan 1993, Riffell & Zimmer 2007) and that velocity fluctuations in typical benthic environments are on the scale of 0.01–0.1 m $s^{-1}$, it is unlikely that sperm motility plays a role in bridging the large initial separation (Levitan 1995, Eckman 1996). Thus, the role of physical stirring by the flow must dominate the aggregation

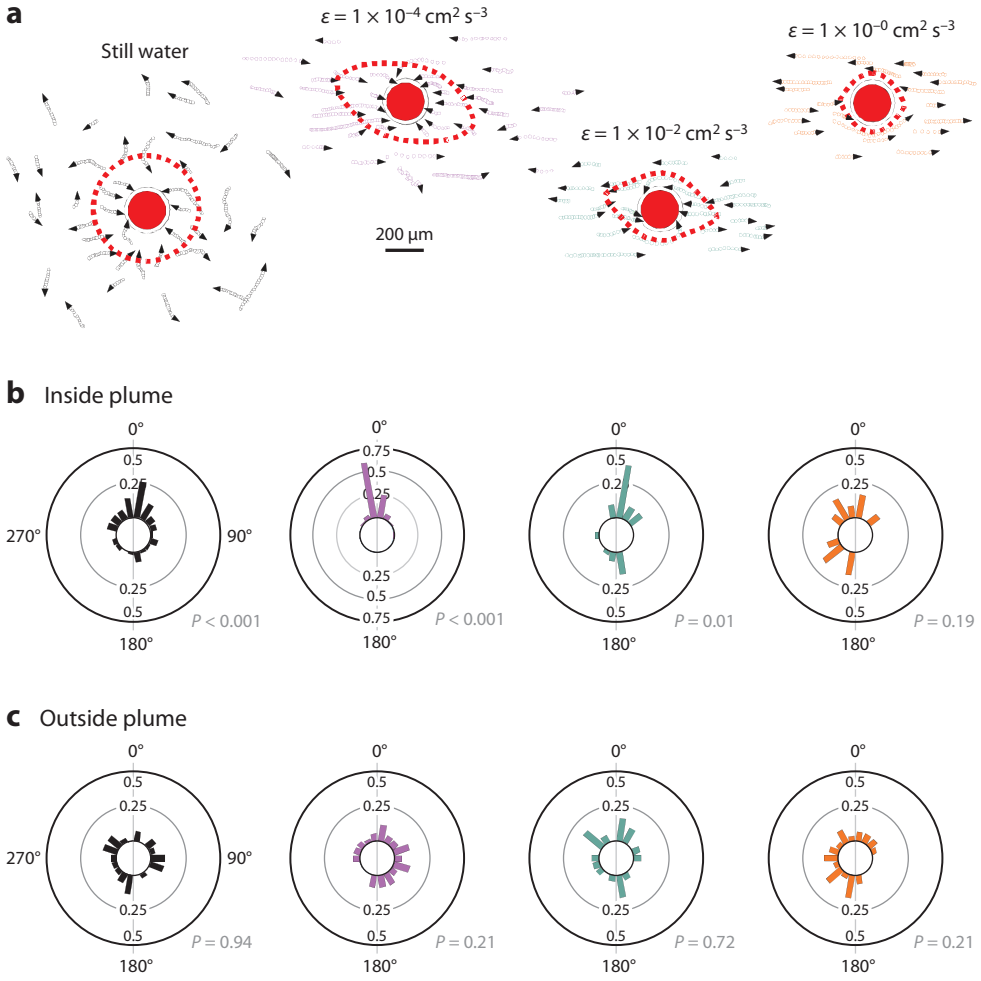


**Figure 7**

(*a*) Representative swimming paths of individual red abalone sperm surrounding conspecific eggs in filtered seawater as a function of shear (with $\varepsilon$ denoted in units of $cm^2\ s^{-3}$). For each experimental treatment, a red dashed line denotes the predicted behavioral threshold concentration. This line demarcates the theoretical active space (i.e., closer to the egg) from the inactive space (i.e., farther from the egg) of an attractant plume. Active space was defined as the portion of a plume maintaining L-tryptophan greater than the threshold level that caused faster sperm swimming speed and orientation with respect to a chemical gradient. Small circles are successive digital images of sperm heads captured at 0.033-s intervals, and each arrowhead denotes the direction of travel for an individual cell. (*b*,*c*) Orientation rosettes showing the distributions of directional tracks by sperm populations positioned inside (panel *b*) or outside (panel *c*) the active space of hypothesized tryptophan plumes. Sperm moving directly toward an egg would follow a 0° heading. A Rayleigh test (*z* value) was used to compare each mean direction against a uniform circular distribution and to calculate the *P* value. Adapted from Zimmer & Riffell (2011).

process at large scales. Although turbulent mixing ultimately has the deleterious effect of diluting gamete concentrations, a number of large-scale turbulent flow processes can aggregate gametes at intermediate timescales before dilution takes place (as reviewed in Section 5). And although gametes are at the mercy of physical processes at this stage, biological properties of the gametes like their size, buoyancy, and matrix rheology may enhance the physical aggregation processes. Physical stirring processes associated with the instantaneous structure of the flow combine with biological properties of the gametes to produce an aggregation that bridges the initial separation imposed by the adults. This first step takes the gametes from the meter to the millimeter scale, from the eddy to the Kolmogorov scale, from the turbulence to the simple shear scale, and from the stirring to the swimming scale.

Although aggregation by physical stirring brings gametes close to one another, it generally does not promote actual contact, which requires the gametes to move across streamlines. Thus, the system necessarily transitions from being physically to biologically dominated at these scales. Sperm motility and taxis may be envisioned as an evolutionary adaptation that provides the necessary cross-streamline mixing (at gamete scales) that solute diffusion provides (at molecular scales) for traditional reaction systems. The small-scale processes of chemoattractant plumes, sperm motility, and sperm taxis reviewed in Section 6 are essential to efficiently bridging the final distance separating the gametes.

The efficacy of the broadcast-spawning process seems, then, to rely on a hierarchical set of protocols based largely on spatial scale. The system transitions from one that is controlled largely by physics at the largest scale to one that relies on biological processes at the smallest scale. What seems clear in a holistic sense, however, is that this fertilization strategy is absolutely dependent on the instantaneous physical processes that initiate the aggregation at large scales, and that without them, the strategy would fail.



## DISCLOSURE STATEMENT

The authors are not aware of any affiliations, memberships, funding, or financial holdings that might be perceived as affecting the objectivity of this review.

## ACKNOWLEDGMENTS

This review was supported by awards from the National Science Foundation (OCE 08-49695 and PHY 12-05816 to J.P.C., and IOS 08-20645 and DBI 11-21692 to R.K.Z.). J.P.C. thanks Michael Soltys for the use of unpublished data in **Figure 5**. R.K.Z. thanks Cheryl Ann Zimmer for many stimulating ideas and excellent editorial assistance.

## LITERATURE CITED

Abelson A, Denny M. 1997. Settlement of marine organisms in flow. *Annu. Rev. Ecol. Syst.* 28:317–39

Atkinson OS, Yund PO. 1996. The effect of variation in population density on male fertilization success in a colonial ascidian. *J. Exp. Mar. Biol. Ecol.* 195:111–23

Babcock RC, Mundy CN, Whitehead D. 1994. Sperm diffusion models and in situ confirmation of long-distance fertilization in the free-spawning asteroid *Acanthaster planci*. *Biol. Bull.* 186:17–28

Babiano A, Cartwright JHE, Piro O, Provenzale A. 2000. Dynamics of a small neutrally buoyant sphere in a fluid and targeting in Hamiltonian systems. *Phys. Rev. Lett.* 84:5764–67

Bandi MM, Cressman JR, Goldburg WI. 2008. Test of the fluctuation relation in Lagrangian turbulence on a free surface. *J. Stat. Phys.* 130:27–38

Barry JP. 1989. Reproductive response of a marine annelid to winter storms: an analog to fire adaptation in plants? *Mar. Ecol. Prog. Ser.* 54:99–107
Bartok W, Mason SG. 1957. Particle motions in sheared suspensions: V. Rigid rods and collisions of spheres. *J. Colloid Interface Sci.* 12:243–263
Benzie JAH, Dixon P. 1994. The effects of sperm concentration, sperm:egg ratio, and gamete age on fertilization success in crown-of-thorns starfish (*Acanthaster planci*) in the laboratory. *Biol. Bull.* 186:139–52
Boffetta G, Davoudi J, De Lillo F. 2006. Multifractal clustering of passive tracers on a surface flow. *Europhys. Lett.* 74:62–68
Boffetta G, Davoudi J, Eckhardt B, Schumacher J. 2004. Lagrangian tracers on a surface flow: the role of time correlations. *Phys. Rev. Lett.* 93:134501
Bolton TF, Thomas FI, Leonard CN. 2000. Maternal energy investment in eggs and jelly coats surrounding eggs of the echinoid *Arbacia punctulata*. *Biol. Bull.* 199:1–5
Caley MJ, Carr MH, Hixon MA, Hughes TP, Jones GP, Menge BA. 1996. Recruitment and the local dynamics of open marine populations. *Annu. Rev. Ecol. Syst.* 27:477–500
Claereboudt M. 1999. Fertilization success in spatially distributed populations of benthic free-spawners: a simulation model. *Ecol. Model.* 121:221–33
Coma R, Lasker H. 1997. Effects of spatial distribution and reproductive biology on in situ fertilization rates of a broadcast-spawning invertebrate. *Biol. Bull.* 193:20–29
Cox PA, Sethian JA. 1985. Gamete motion, search, and the evolution of anisogamy, oogamy, and chemotaxis. *Am. Nat.* 125:74–101
Crenshaw HC. 1996. A new look at locomotion in microorganisms: rotating and translating. *Am. Zool.* 36:608–18
Cressman JR, Davoudi J, Goldburg WI, Schumacher J. 2004. Eulerian and Lagrangian studies in surface flow turbulence. *New J. Phys.* 6:53
Crimaldi JP. 2008. Planar laser induced fluorescence in aqueous flows. *Exp. Fluids* 44:851–63
Crimaldi JP. 2012. The role of structured stirring and mixing on gamete dispersal and aggregation in broadcast spawning. *J. Exp. Biol.* 215:1031–39
Crimaldi JP, Browning HS. 2004. A proposed mechanism for turbulent enhancement of broadcast spawning efficiency. *J. Mar. Syst.* 49:3–18
Crimaldi JP, Cadwell JR, Weiss JB. 2008. Reaction enhancement of isolated scalars by vortex stirring. *Phys. Fluids* 20:073605
Crimaldi JP, Hartford JR, Weiss JB. 2006. Reaction enhancement of point sources due to vortex stirring. *Phys. Rev. E* 74:016307
Crimaldi JP, Kawakami TR. 2013. Reaction of initially distant scalars in a cylinder wake. *Phys. Fluids* 25:053604
Crimaldi JP, Koseff JR. 2001. High-resolution measurements of the spatial and temporal scalar structure of a turbulent plume. *Exp. Fluids* 31:90–102
Crimaldi JP, Koseff JR. 2006. Structure of turbulent plumes from a momentumless source in a smooth bed. *Environ. Fluid Mech.* 6:573–92
Crimaldi JP, Wiley MB, Koseff JR. 2002. The relationship between mean and instantaneous structure in turbulent passive scalar plumes. *J. Turbul.* 3:N14
Crowe CT, Troutt TR, Chung JN, Davis RW, Moore EF. 1995. A turbulent flow without particle mixing. *Aerosol Sci. Technol.* 22:135–38
Csanady GT, ed. 1973. *Turbulent Diffusion in the Environment*. Boston: Reidel
Danckwerts PV. 1952. The definition and measurement of some characteristics of mixtures. *Appl. Sci. Res. A* 3:279–96
Denissenko P, Falkovich G, Lukaschuk S. 2006. How waves affect the distribution of particles that float on a liquid surface. *Phys. Rev. Lett.* 97:244501
Denny MW, Dairiki J, Distefano S. 1992. Biological consequences of topography on wave-swept rocky shores: I. Enhancement of external fertilization. *Biol. Bull.* 183:220–32
Denny MW, Gaylord B. 2010. Marine ecomechanics. *Annu. Rev. Mar. Sci.* 2:89–114
Denny MW, Nelson EK, Mead KS. 2002. Revised estimates of the effects of turbulence on fertilization in the purple sea urchin, *Strongylocentrotus purpuratus*. *Biol. Bull.* 203:275–77

Denny MW, Shibata MF. 1989. Consequences of surf-zone turbulence for settlement and external fertilization. *Am. Nat.* 134:859–89
Ducasse L, Pumir A. 2008. Intermittent particle distribution in synthetic free-surface turbulent flows. *Phys. Rev. E* 77:066304
Dusenbery DB. 2006. Selection for high gamete encounter rates explains the evolution of anisogamy using plausible assumptions about size relationships of swimming speed and duration. *J. Theor. Biol.* 241:33–38
Eckhardt B, Schumacher J. 2001. Turbulence and passive scalar transport in a free-slip surface. *Phys. Rev. E* 64:016314
Eckman JE. 1996. Closing the larval loop: linking larval ecology to the population dynamics of marine benthic invertebrates. *J. Exp. Mar. Biol. Ecol.* 200:207–37
Farley GS, Levitan DR. 2001. The role of jelly coats in sperm-egg encounters, fertilization success, and selection on egg size in broadcast spawners. *Am. Nat.* 157:626–36
Gaines SD, Bertness MD. 1992. Dispersal of juveniles and variable recruitment in sessile marine species. *Nature* 360:579–80
Gaylord B, Reed DC, Raimondi PT, Washburn L. 2006. Macroalgal spore dispersal in coastal environments: mechanistic insights revealed by theory and experiment. *Ecol. Monogr.* 76:481–502
Gerritsen J, Strickler JR. 1977. Encounter probabilities and community structure in zooplankton: a mathematical model. *J. Fish. Board Can.* 34:73–82
Giese AC, Pearse JS, eds. 1974. *Reproduction of Marine Invertebrates*. New York: Academic
Goldburg WI, Cressman JR, Vörös Z, Eckhardt B, Schumacher J. 2001. Turbulence in a free surface. *Phys. Rev. E* 63:065303
Gray J. 1955. The movement of sea-urchin spermatozoa. *J. Exp. Biol.* 32:775–801
Guasto JS, Rusconi R, Stocker R. 2012. Fluid mechanics of planktonic microorganisms. *Annu. Rev. Fluid Mech.* 44:373–400
Hart DD, Finelli CM. 1999. Physical-biological coupling in streams: the pervasive effects of flow on benthic organisms. *Annu. Rev. Ecol. Syst.* 30:363–95
Hasegawa D, Yamazaki H, Lueck RG, Seuront L. 2004. How islands stir and fertilize the upper ocean. *Geophys. Res. Lett.* 31:4
Havenhand JN. 1993. Egg to juvenile period, generation time, and the evolution of larval type in marine invertebrates. *Mar. Ecol. Prog. Ser.* 97:247–60
Hill JC. 1976. Homogeneous turbulent mixing with chemical reaction. *Annu. Rev. Fluid Mech.* 8:135–61
Hill PS, McCave IN. 2001. Suspended particle transport in benthic boundary layers. In *The Benthic Boundary Layer: Transport Processes and Biogeochemistry*, ed. BP Boudreau, BB Jørgensen, pp. 78–103. Oxford, UK: Oxford Univ. Press
Hill PS, Nowell ARM. 1995. Comparison of two models of aggregation in continental-shelf bottom boundary layers. *J. Geophys. Res.* 100:22749–63
Hill PS, Nowell ARM, Jumars PA. 1992. Encounter rate by turbulent shear of particles similar in diameter to the kolmogorov scale. *J. Mar. Res.* 50:643–68
Hodgson AN, Le Quesne WJF, Hawkins SJ, Bishop JDD. 2007. Factors affecting fertilization success in two species of patellid limpet (Mollusca: Gastropoda) and development of fertilization kinetics models. *Mar. Biol.* 150:415–26
Hoekstra RF. 1987. The evolution of sexes. *Exp. Suppl.* 55:59–91
Hughes TP, Baird AH, Dinsdale EA, Moltschaniwskyj NA, Pratchett MS, et al. 2000. Supply-side ecology works both ways: the link between benthic adults, fecundity, and larval recruits. *Ecology* 81:2241–49
Inamdar MV, Kim T, Chung Y-KK, Was AM, Xiang X, et al. 2007. Assessment of sperm chemokinesis with exposure to jelly coats of sea urchin eggs and resact: a microfluidic experiment and numerical study. *J. Exp. Biol.* 210:3805–20
Jackson GA, Burd AB. 1998. Aggregation in the marine environment. *Environ. Sci. Technol.* 32:2805–14
Jaeckle WB. 1995. Variation in the size, energy content, and biochemical composition of invertebrate eggs: correlates to the mode of larval development. In *Ecology of Marine Invertebrate Larvae*, ed. L McEdward, pp. 49–89. Boca Raton, FL: CRC
Jeffery GB. 1922. The motion of ellipsoidal particles immersed in a viscous fluid. *Proc. R. Soc. Lond. A* 102:161–79

Jumars PA, Trowbridge JH, Boss E, Karp-Boss L. 2009. Turbulence-plankton interactions: a new cartoon. *Mar. Ecol.* 30:133–50
Karp-Boss L, Boss E, Jumars PA. 1996. Nutrient fluxes to planktonic osmotrophs in the presence of fluid motion. *Oceanogr. Mar. Biol.* 34:71–108
Karp-Boss L, Jumars PA. 1998. Motion of diatom chains in steady shear flow. *Limnol. Oceanogr.* 43:1767–73
Kiørboe T, Saiz E. 1995. Planktivorous feeding in calm and turbulent environments, with emphasis on copepods. *Mar. Ecol. Prog. Ser.* 122:135–45
Krug PJ, Riffell JA, Zimmer RK. 2009. Endogenous signaling pathways and chemical communication between sperm and egg. *J. Exp. Biol.* 212:1092
Kumar S, Gupta R, Banerjee S. 1998. An experimental investigation of the characteristics of free-surface turbulence in channel flow. *Phys. Fluids* 10:437
Larson RJ. 1992. Riding langmuir circulations and swimming in circles: a novel form of clustering behavior by the scyphomedusa *Linuche unguiculata*. *Mar. Biol.* 112:229–35
Lauzon-Guay JS, Scheibling RE. 2007. Importance of spatial population characteristics on the fertilization rates of sea urchins. *Biol. Bull.* 212:195–205
Lazier JRN, Mann KH. 1989. Turbulence and the diffusive layers around small organisms. *Deep-Sea Res. A* 36:1721–33
Levitan DR. 1993. The importance of sperm limitation to the evolution of egg size in marine invertebrates. *Am. Nat.* 141:517–36
Levitan DR. 1995. The ecology of fertilization in free-spawning invertebrates. In *Ecology of Marine Invertebrate Larvae*, ed. L McEdward, pp. 123–56. Boca Raton, FL: CRC
Levitan DR. 2005. The distribution of male and female reproductive success in a broadcast spawning marine invertebrate. *Integr. Comp. Biol.* 45:848–55
Levitan DR. 2006. The relationship between egg size and fertilization success in broadcast-spawning marine invertebrates. *Integr. Comp. Biol.* 46:298–311
Levitan DR, Sewell MA, Chia F. 1991. Kinetics of fertilization in the sea urchin *Strongylocentrotus franciscanus*: interaction of gamete dilution, age, and contact time. *Biol. Bull.* 181:371–78
Levitan DR, Young CM. 1995. Reproductive success in large populations: empirical measures and theoretical predictions of fertilization in the sea biscuit *Clypeaster rosaceus*. *J. Exp. Mar. Biol. Ecol.* 190:221–41
Lewis DM. 2003. Planktonic encounter rates in homogeneous isotropic turbulence: the case of predators with limited fields of sensory perception. *J. Theor. Biol.* 222:73–97
Lewis JR. 1986. Latitudinal trends in reproduction, recruitment and population characteristics of some rocky littoral molluscs and cirripedes. *Hydrobiologia* 142:1–13
Lukaschuk S, Denissenko P, Falkovich G. 2006. Clustering of floating particles by surface waves. *J. Low Temp. Phys.* 145:297–310
Luttikhuizen PC, Honkoop PJC, Drent J, van der Meer J. 2004. A general solution for optimal egg size during external fertilization, extended scope for intermediate optimal egg size and the introduction of Don Ottavio "tango." *J. Theor. Biol.* 231:333–43
Maier I, Müller DG. 1986. Sexual pheromones in algae. *Biol. Bull.* 170:145–75
Maldonado EM, Latz MI. 2011. Species-specific effects of fluid shear on grazing by sea urchin larvae: comparison of experimental results with encounter-model predictions. *Mar. Ecol. Prog. Ser.* 436:119–30
Mann KH, Lazier JRN. 1996. *Dynamics of Marine Ecosystems: Biological-Physical Interactions in the Ocean*. Cambridge, MA: Blackwell Sci. 2nd ed.
Marshall DJ. 2002. In situ measures of spawning synchrony and fertilization success in an intertidal, free-spawning invertebrate. *Mar. Ecol. Prog. Ser.* 236:113–19
Marshall DJ, Bolton TF, Keough MJ. 2003. Offspring size affects the post-metamorphic performance of a colonial marine invertebrate. *Ecology* 84:3131–37
Maxey MR. 1990. On the advection of spherical and non-spherical particles in a non-uniform flow. *Philos. Trans. R. Soc. Lond. A* 333:289–307
McEdward LR, Miner BG. 2006. Estimation and interpretation of egg provisioning in marine invertebrates. *Integr. Comp. Biol.* 46:224–32

McEuen FS. 1988. Spawning behaviors of northeast Pacific sea cucumbers (Holothuroidea: Echinodermata). *Mar. Biol.* 98:565–85

Metaxas A, Scheibling RE, Young CM. 2002. Estimating fertilization success in marine benthic invertebrates: a case study with the tropical sea star *Oreaster reticulatus*. *Mar. Ecol. Prog. Ser.* 226:87–101

Meunier P, Villermaux E. 2003. How vortices mix. *J. Fluid Mech.* 476:213–22

Millar RB, Anderson MJ. 2003. The kinetics of monospermic and polyspermic fertilization in free-spawning marine invertebrates. *J. Theor. Biol.* 224:79–85

Miller RL. 1985. Sperm chemo-orientation in the metazoa. In *Biology of Fertilization*, Vol. 2, *Biology of the Sperm*, ed. CB Metz, A Monroy, pp. 275–337. New York: Academic

Miller RL, Vogt R. 1996. An N-terminal partial sequence of the 13 kDa *Pycnopodia helianthoides* sperm chemoattractant "startrak" possesses sperm-attracting activity. *J. Exp. Biol.* 199:311–18

Moláček J, Denny M, Bush JWM. 2011. The fine art of surfacing: its efficacy in broadcast spawning. *J. Theor. Biol.* 7:40–47

Morgan SG, Christy JH. 1994. Plasticity, constraint, and optimality in reproductive timing. *Ecology* 75:2185–203

Mozingo NM, Vacquier VD, Chandler DE. 1995. Structural features of the abalone egg extracellular matrix and its role in gamete interaction during fertilization. *Mol. Reprod. Dev.* 41:493–502

Niederkorn TC, Ottino JM. 1994. Chaotic mixing of shear-thinning fluids. *AIChE J.* 40:1782–93

Nowell ARM, Jumars PA. 1984. Flow environments of aquatic benthos. *Annu. Rev. Ecol. Syst.* 15:303–28

Oliver JK, Willis BL. 1987. Coral-spawn slicks in the Great Barrier Reef: preliminary observations. *Mar. Biol.* 94:521–29

Olson JH, Xiang X, Ziegert T, Kittelson A, Rawls A, et al. 2001. Allurin, a 21-kDa sperm chemoattractant from *Xenopus* egg jelly, is related to mammalian sperm-binding proteins. *Sci. Signal.* 98:11205

Pearson GA, Brawley SH. 1996. Reproductive ecology of *Fucus distichus* (phaeophyceae): an intertidal alga with successful external fertilization. *Mar. Ecol. Prog. Ser.* 143:211–23

Pennington JT. 1985. The ecology of fertilization of echinoid eggs: the consequences of sperm dilution, adult aggregation, and synchronous spawning. *Biol. Bull.* 169:417–30

Picken GB, Allan D. 1983. Unique limpet spawning behavior. *Nature* 305:472

Podolsky RD. 2001. Evolution of egg target size: an analysis of selection on correlated characters. *Evolution* 55:2470–78

Podolsky RD. 2004. Life-history consequences of investment in free-spawned eggs and their accessory coats. *Am. Nat.* 163:735–53

Rahman S, Webster DR. 2005. The effect of bed roughness on scalar fluctuations in turbulent boundary layers. *Exp. Fluids* 38:372–84

Reade WC, Collins LR. 2000. Effect of preferential concentration on turbulent collision rates. *Phys. Fluids* 12:2530

Reigada R, Sagués F, Sancho JM. 2001. Inertial effects on reactive particles advected by turbulence. *Phys. Rev. E* 64:026307

Reinhart D, Ridgway J, Chandler DE. 1998. *Xenopus laevis* fertilisation: analysis of sperm motility in egg jelly using video light microscopy. *Zygote* 6:173–82

Riffell JA, Krug PJ, Zimmer RK. 2002. Fertilization in the sea: the chemical identity of an abalone sperm attractant. *J. Exp. Biol.* 205:1439–50

Riffell JA, Zimmer RK. 2007. Sex and flow: the consequences of fluid shear for sperm egg interactions. *J. Exp. Biol.* 210:3644–60

Rothschild BJ, Osborn TR. 1988. Small-scale turbulence and plankton contact rates. *J. Plankton Res.* 10:465

Sandulescu M, López C, Hernández-García E, Feudel U. 2007. Plankton blooms in vortices: the role of biological and hydrodynamic timescales. *Nonlinear Process. Geophys.* 14:443–54

Schumacher J, Eckhardt B. 2002. Clustering dynamics of Lagrangian tracers in free-surface flows. *Phys. Rev. E* 66:017303

Shen L, Zhang X, Yue DKP, Triantafyllou GS. 1999. The surface layer for free-surface turbulent flows. *J. Fluid Mech.* 386:167–212

Shraiman BI, Siggia ED. 2000. Scalar turbulence. *Nature* 405:639–46

Singh P, Joseph DD. 2005. Fluid dynamics of floating particles. *J. Fluid Mech.* 530:31–80
Soltys MA, Crimaldi JP. 2011. Scalar interactions between parallel jets measured using a two-channel PLIF technique. *Exp. Fluids* 50:1625–32
Spehr M, Gisselmann G, Poplawski A, Riffell JA, Wetzel CH, et al. 2003. Identification of a testicular odorant receptor mediating human sperm chemotaxis. *Science* 299:2054–58
Squires KD, Eaton JK. 1991. Preferential concentration of particles by turbulence. *Phys. Fluids A* 3:1169
Squires KD, Yamazaki H. 1995. Preferential concentration of marine particles in isotropic turbulence. *Deep-Sea Res. I* 42:1989–2004
Strathmann RR. 1985. Feeding and nonfeeding larval development and life-history evolution in marine invertebrates. *Annu. Rev. Ecol. Syst.* 16:339–61
Styan CA. 1998. Polyspermy, egg size, and the fertilization kinetics of free-spawning marine invertebrates. *Am. Nat.* 152:290–97
Styan CA, Butler AJ. 2000. Fitting fertilisation kinetics models for free-spawning marine invertebrates. *Mar. Biol.* 137:943–51
Svane IB, Havenhand JN. 1993. Spawning and dispersal in *Ciona intestinalis* (L.). *Mar. Ecol.* 14:53–66
Tang L, Wen F, Yang Y, Crowe CT, Chung JN, Troutt TR. 1992. Self-organizing particle dispersion mechanism in a plane wake. *Phys. Fluids A* 4:2244–51
Thomas FIM. 1994a. Physical properties of gametes in three sea urchin species. *J. Exp. Biol.* 194:263–84
Thomas FIM. 1994b. Transport and mixing of gametes in three free-spawning polychaete annelids, *Phragmatopoma californica* (Fewkes), *Sabellaria cementarium* (Moore), and *Schizobranchia insignis* (Bush). *J. Exp. Mar. Biol. Ecol.* 179:11–27
Thorpe SA. 2004. Langmuir circulation. *Annu. Rev. Fluid Mech.* 36:55–79
Underwood AJ, Keough MJ. 2001. Supply-side ecology: the nature and consequences of variations in recruitment of intertidal organisms. In *Marine Community Ecology*, ed. MD Bertness, SD Gaines, ME Hay, pp. 183–200. Sunderland, MA: Sinauer
Vacquier VD, Moy GW. 1997. The fucose sulfate polymer of egg jelly binds to sperm REJ and is the inducer of the sea urchin sperm acrosome reaction. *Dev. Biol.* 192:125–35
Villermaux E, Duplat J. 2003. Mixing as an aggregation process. *Phys. Rev. Lett.* 91:184501
Visser AW, Kiørboe T. 2006. Plankton motility patterns and encounter rates. *Oecologia* 148:538–46
Vogel H, Czihak G, Chang P, Wolf W. 1982. Fertilization kinetics of sea urchin eggs. *Math. Biosci.* 58:189–216
Ward GE, Brokaw CJ, Garbers DL, Vacquier VD. 1985. Chemotaxis of *Arbacia punctulata* spermatozoa to resact, a peptide from the egg jelly layer. *J. Cell Biol.* 101:2324–29
Warhaft Z. 2000. Passive scalars in turbulent flows. *Annu. Rev. Fluid Mech.* 32:203–40
Webster DR, Rahman S, Dasi LP. 2003. Laser-induced fluorescence measurements of a turbulent plume. *J. Eng. Mech.* 129:1130–37
Webster DR, Weissburg MJ. 2009. The hydrodynamics of chemical cues among aquatic organisms. *Annu. Rev. Fluid Mech.* 41:73–90
Yoshida M, Murata M, Inaba K, Morisawa M. 2002. A chemoattractant for ascidian spermatozoa is a sulfated steroid. *Proc. Natl. Acad. Sci. USA* 99:14831
Yund PO. 2000. How severe is sperm limitation in natural populations of marine free-spawners? *Trends Ecol. Evol.* 15:10–13
Yund PO, Meidel SK. 2003. Sea urchin spawning in benthic boundary layers: Are eggs fertilized before advecting away from females? *Limnol. Oceanogr.* 48:795–801
Zimmer RK, Riffell JA. 2011. Sperm chemotaxis, fluid shear, and the evolution of sexual reproduction. *Proc. Natl. Acad. Sci. USA* 108:13200–5

Annual Review of
Marine Science

Volume 6, 2014

# Contents

Shedding Light on the Sea: André Morel's Legacy to Optical Oceanography
*David Antoine, Marcel Babin, Jean-François Berthon, Annick Bricaud, Bernard Gentili, Hubert Loisel, Stéphane Maritorena, and Dariusz Stramski* ..... 1

Benthic Exchange and Biogeochemical Cycling in Permeable Sediments
*Markus Huettel, Peter Berg, and Joel E. Kostka* ..... 23

Contemporary Sediment-Transport Processes in Submarine Canyons
*Pere Puig, Albert Palanques, and Jacobo Martín* ..... 53

El Niño Physics and El Niño Predictability
*Allan J. Clarke* ..... 79

Turbulence in the Upper-Ocean Mixed Layer
*Eric A. D'Asaro* ..... 101

Sounds in the Ocean at 1–100 Hz
*William S.D. Wilcock, Kathleen M. Stafford, Rex K. Andrew, and Robert I. Odom* .. 117

The Physics of Broadcast Spawning in Benthic Invertebrates
*John P. Crimaldi and Richard K. Zimmer* ..... 141

Resurrecting the Ecological Underpinnings of Ocean Plankton Blooms
*Michael J. Behrenfeld and Emmanuel S. Boss* ..... 167

Carbon Cycling and Storage in Mangrove Forests
*Daniel M. Alongi* ..... 195

Ocean Acidification in the Coastal Zone from an Organism's Perspective: Multiple System Parameters, Frequency Domains, and Habitats
*George G. Waldbusser and Joseph E. Salisbury* ..... 221

Climate Change Influences on Marine Infectious Diseases: Implications for Management and Society
*Colleen A. Burge, C. Mark Eakin, Carolyn S. Friedman, Brett Froelich, Paul K. Hershberger, Eileen E. Hofmann, Laura E. Petes, Katherine C. Prager, Ernesto Weil, Bette L. Willis, Susan E. Ford, and C. Drew Harvell* ..... 249

Microbially Mediated Transformations of Phosphorus in the Sea: New Views of an Old Cycle
*David M. Karl* ..... 279

The Role of B Vitamins in Marine Biogeochemistry
*Sergio A. Sañudo-Wilhelmy, Laura Gómez-Consarnau, Christopher Suffridge, and Eric A. Webb* ..... 339

Hide and Seek in the Open Sea: Pelagic Camouflage and Visual Countermeasures
*Sönke Johnsen* ..... 369

Antagonistic Coevolution of Marine Planktonic Viruses and Their Hosts
*Jennifer B.H. Martiny, Lasse Riemann, Marcia F. Marston, and Mathias Middelboe* ..... 393

Tropical Marginal Seas: Priority Regions for Managing Marine Biodiversity and Ecosystem Function
*A. David McKinnon, Alan Williams, Jock Young, Daniela Ceccarelli, Piers Dunstan, Robert J.W. Brewin, Reg Watson, Richard Brinkman, Mike Cappo, Samantha Duggan, Russell Kelley, Ken Ridgway, Dhugal Lindsay, Daniel Gledhill, Trevor Hutton, and Anthony J. Richardson* ..... 415

Sea Ice Ecosystems
*Kevin R. Arrigo* ..... 439

The Oceanography and Ecology of the Ross Sea
*Walker O. Smith Jr., David G. Ainley, Kevin R. Arrigo, and Michael S. Dinniman* ..... 469

**Errata**

An online log of corrections to *Annual Review of Marine Science* articles may be found at http://www.annualreviews.org/errata/marine